Spring 5-14-2012

In Situ Surface Voltage Measurements of Dielectrics Under Electron Beam Irradiation

Joshua L. Hodges
Utah State University

JR Dennison
Utah State University

Justin Dekany
Utah State University

Gregory Wilson
Utah State University

Amberly Evans Jensen
Utah State University

Alec Sim
Utah State University & Irving Valley College

In Situ Surface Voltage Measurements of Dielectrics Under Electron Beam Irradiation

USU Materials Physics Group

Joshua L. Hodges, JR Dennison, Justin Dekany, Gregory Wilson, Amberly Evans, and Alec M. Sim

Utah State University, Logan, Utah 84322-4415

Phone: (435) 760-7816, FAX: (435) 797-2492, E-mail:joshuahodges@hill.af.mill

12th Spacecraft Charging Technology Conference, 14-18 May,2012, Kitakyushu,Japan

Design Goals

When designing an instrument, the physical parameters of the measurements being made drive the design of the apparatus. The constraints on these parameters (actual values shown in green) are based on the electrical properties of typical spacecraft materials.

- Range: <1 V based on breakdown voltages of semiconductors to >10 kV, for breakdown voltages of insulators (1.2 V -30 kV)
- Resolution: ~10% of lower range (0.2 V)
- Response Speed: ~1-10 seconds based on low resistivity response time and minimum time for environmental changes (7 sec)
- Stability: >10^5 seconds based on typical insulator decay times (~∞ due to self calibration)

Actual instrument parameters are green

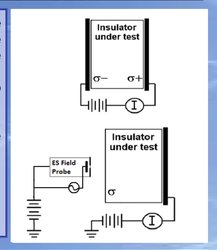

Characterization and Calibration

Extensive testing helped develop an understanding of all effects factoring into Eq.(1), that converts probe voltage to a sample voltage.

$$V_{sample} = CF\left[\begin{array}{c} V_{probe} - V_{offset} - V_{elec_o}\left(1 + V_{elec}\left(t - t_d\right)\right) - \\ V_{drift_o}\left(1 - e^{\frac{-(t-t_d)}{\tau_d}}\right) - \left(1 - e^{\beta V_{probe}}\right)\left(1 - e^{\frac{-(t-t_v)}{\tau_v}}\right) \end{array}\right] \quad (1)$$

(Top) Repeated linear calibration measurements of the large electrode give a calibration factor of 1084±0.5 V_{sample} /V_{probe} with a correlation coefficient of 1.000. (Middle) Raw data from an *in situ* voltage ramp run, to determine ground drift, voltage drift, and calibration factor curves. (Bottom) Multiple ground drift measurements show the need for a self calibration. Two runs show two distinctly different curves with time constants of 1325±32 seconds and 1450±36 seconds. With our unique self calibration the errors due to reproducibility of these curves are negligible.

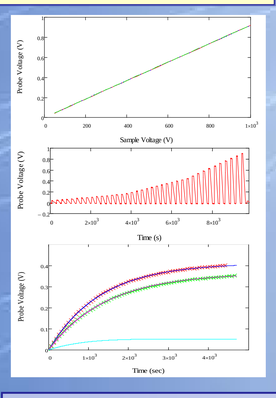

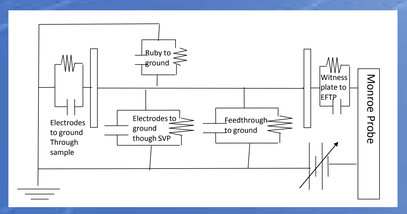

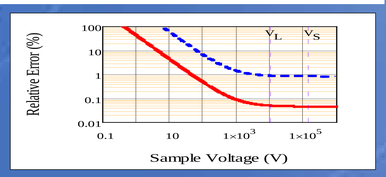

(Top) An idealized electrical schematic developed to treat each leakage path as an RC circuit. Time dependant errors in Eq.(1) are negligible for elapsed times after ground calibration of <150 s. Terms in Eq.(1) are identified in the table below. (Bottom) An equation for the approximant relative error for large (blue) and small (red) electrodes was built based on Eq.(1) and the table below.

$$\frac{\Delta V_{sample}}{V_{sample}} = \frac{\Delta CF}{CF} + 2\frac{\Delta V_{probe}}{V_{probe}}$$

CF	Linear voltage calibration compares sample voltage to probe voltage	$\frac{V_{probe}}{V_{sample}}$	(1084.5±0.5) L.E. (14900±125) S.E.
V_{elec}	Offset of electronics value is enveloped in the Probe offset and adjusted by user on front panel of EFTP controller	$V_{offset} + V_{elec_o}[1 + V_{elec}(t - t_d)]$	(1.0±.8)mV
V_{elec_o}	Drift of the EFTP controller, value is small on typical timescales of measurements		Typically (2.0±0.2)mV/hr
V_{offset}	Probe Voltage Offset, determined from the exponential fit to the drift data		Measured each run (13±3)mV
V_{drift_o}	Probe ground drift rate, determined from the exponential fit to the drift data	$V_{drift_o}\left(1 - e^{\frac{-(t-t_d)}{\tau_d}}\right)$	Measured each run (32±0.8)mV/s
τ_d	Time constant of the probe ground drift, determined from the exponential fit to the drift data		Measured each run typical on the order of (1400±100) s
β	Sample voltage drift slope, determined from the exponential fit to the drift data	$\left(1 - e^{\beta V_{probe}}\right)\left(1 - e^{\frac{-(t-t_v)}{\tau_v}}\right)$	(2.5±0.4) 1/V
τ_v	Time constant of sample voltage drift, determined from the exponential fit to the drift data		(-6x10^6±2x10^6) mV/s

Abstract

New instrumentation has been developed for non-contact, *in vacuo* measurements of the electron beam-induced surface voltage as a function of time and position for non-conductive spacecraft materials in a simulated space environment. Used in conjunction with the capabilities of an existing ultrahigh vacuum electron emission analysis chamber, the new instrumentation facilitates measurements of charge accumulation, bulk resistivity, effects of charge depletion and accumulation on yield measurements, electron induced electrostatic breakdown potentials, radiation induced conductivity effects, and the radial dispersion of surface voltage.

The novel system uses two movable capacitive sensor electrodes that can be swept across the sample to measure surface charge distributions on samples, using a non-contact method that does not dissipate sample charge. Design details, calibration and characterization measurements of the system are presented, for a surface voltage range from <1 V to >30 kV, voltage resolution <1 V, and spatial resolution <1.5 mm. Extensive characterization tests with externally biased conductors were performed to calibrate the system and determine the instrument stability, sensitivity, accuracy, range, spatial resolution and temporal response.

Two types of measurements have been made on two prototypical polymeric spacecraft materials, low density polyethylene (LDPE) and polyimide (Kapton HN™) to illustrate the research capabilities of the new system. First, surface voltage measurements were made using a pulsed electron beam, while periodically measuring the surface voltage. Second, post charging measurements of the surface voltage were conducted, as deposited charge dissipated to a grounded substrate. Theoretical models for sample charging and discharge are outlined to predict the time, temperature, and electric field dependence of the sample net surface voltage. The good agreement between the fitting parameters of the model is discussed and the corresponding physical parameters determined from the literature and measurements by related techniques.

Design of the Instrumentation

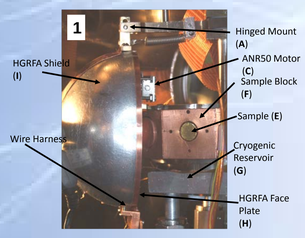

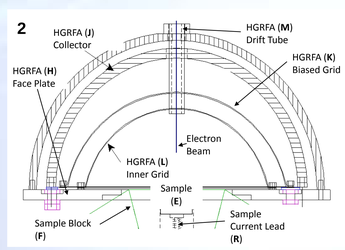

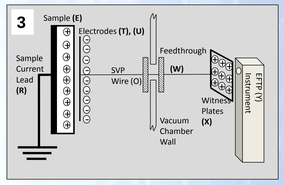

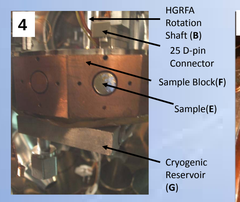

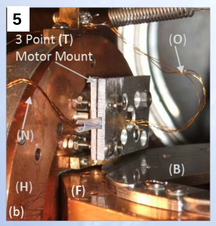

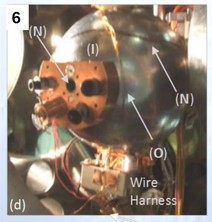

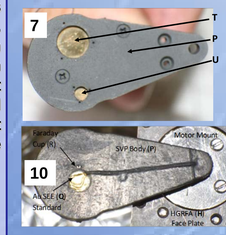

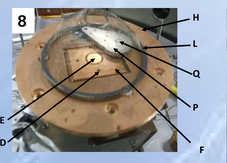

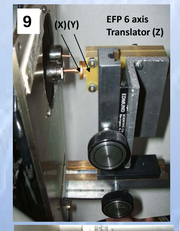

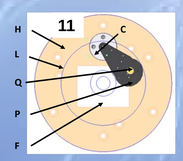

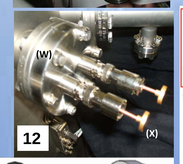

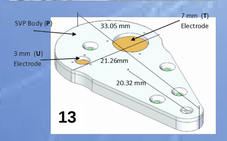

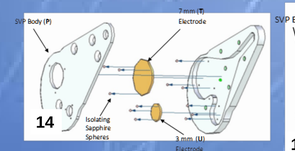

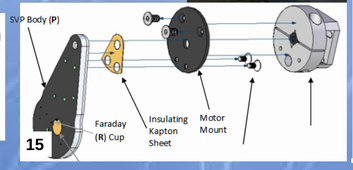

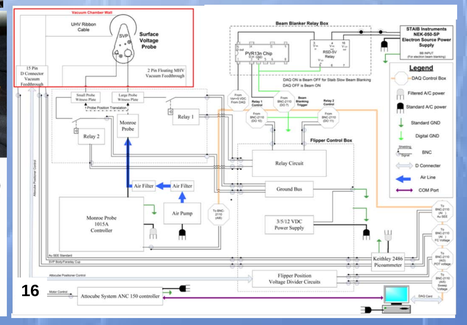

Legend

A. HGRFA Hinged Mount
B. Sample Carousel/HGRFA Rotation Shaft
C. UHV Stepper Motor
D. Sample Block Faraday Cup
E. Sample (10 mm)
F. Sample Block
G. Cryogen Reservoir
H. HGRFA Face Plate
I. HGRFA Hemispherical Shield
J. HGRFA Collector
K. HGRFA Bias Grid
L. HGRFA Inner Grid
M. HGRFA Drift Tube
N. Electron Flood Gun
O. LED Light Source
P. Surface Voltage Probe (SVP)
Q. Au Electron Emission Standard
R. Sample Current Lead
S. SVP Faraday Cup
T. SVP 7 mm Diameter Au Electrode
U. SVP 3 mm Diameter Au Electrode
V. SVP Wiring Channel
W. EFTP Vacuum Feedthrough
X. EFTP Witness Plate
Y. Electrostatic Field Probe
Z. Probe XYZ Translator

Hemispherical Grid Retarding Field Analyzer (HGRFA) Figs. 1-6
(1) Photograph of sample stage and HGRFA detector (side view). (2) Cross section of HGRFA. (3) NEEDS A CAPTION HERE (4) Photograph of sample stage showing sample and cooling reservoir. (5) Side view of the mounting of the stepper motor. (6) Isometric view of the HGRFA detailing the flood gun, optical ports, and wire harness.

Surface Voltage Probe (SVP) Figs. 7-16
(7) Photograph of sample side of surface voltage probe assembly. (8)Photograph of the SVP with the collecting hemisphere removed. (9) 6 axis EFP translation stage mounted parallel to a witness plate. (10) Photograph of Au SEE standard and Aquadag surface of the SVP. (11) Diagram of HGRFA interior with SVP, looking toward the sample. (12) Air side of SVP with the witness plate feedthrough and connectors. (13) Overall dimensions of SVP with center of gravity indicated. (14) Exploded view of SVP internal parts. (15) Exploded view of SVP motor assembly. (16) Surface voltage probe block diagram.

Experimental Applications

Charge Accumulation from Incident Electron Flux.

Figure A shows the surface voltage response of LDPE during irradiation by a non-penetrating electron beam at ~ 5keV with a fluency of ~ 1.1 nA/cm^2. The net charge deposited in the material is proportional to the surface voltage. The equilibrium voltage is established as charge increases filling the density of trap states N_t in the material. The relation between the surface voltage, injection current J_0, capture cross section *s*, range *r*, permittivity ε, and total density of states is given by Eq. A, where *K* and *m* are constants related to the quantum nature of the material interface [A Sim].

The residual plot shows excellent agreement with error of the fit ranging from 3% to 10%, with very good agreement between the literature and fitted material parameters (see Table).

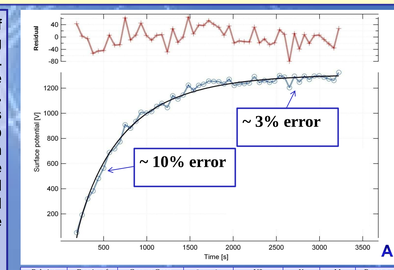

Relative Permittivity $\epsilon^*\epsilon_0$	Density of states [1/cm^3]	Capture Cross section [cm^2]	Sample thickness [μm]	V0 [V]	K [1/s]^m	M [none]	Range r [m]
2.6	2.029e+17	1.498e-14	27.4	1311	33.315	0.129	1.0e-6

$$V_s(t) = \frac{rdq}{\epsilon}N_t\left(1 - exp\left[\frac{-sJ_0t\left[1 + \frac{Kt^{1-m}}{1-m}\right]}{q}\right]\right) \quad A$$

Charge Dissipation of Highly Insulating Materials.

Figure B shows the surface decay of Kapton after cessation of charging. Voltage decays as charge leaks from the trapped states to the ground plane. The surface potential $V_s(t)$ (Eq. B) is proportional to the initial voltage V(0), de-trapping rate, trapping rate, mobility, and the dispersion parameter $\alpha=T/T_0$, where T_0 defines the spread of traps in the mobility gap.

The residual plot shows excellent agreement between the model and data, with residuals of between 3% and 5%. Again, there is very good agreement between the literature and fitted material parameters (see Table).

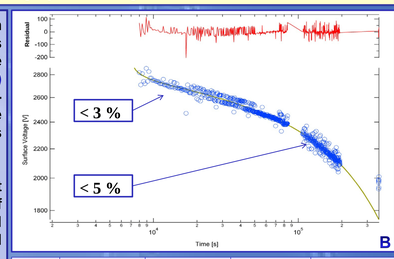

V(0) [V]	Mobility μ_0 [m^2/Vs]	Release rate ν_r [1/s]	Trap rate ν_t [1/s]	α [none]
2827	6.981-17	4.34E-05	7.32E-04	.335

$$V_s(t) = V(0)\left(1 - \frac{\mu_0 V(0)}{2d^2(\nu_r+\nu_t)}\left(\nu_r t + \frac{\nu_t}{\nu_r+\nu_t}\left(1 - e^{-(\nu_r+\nu_t)t}\right)\right) - \frac{\mu_0 V(0) sin[\alpha\pi]}{2d^2\alpha^2\pi}\left(\frac{1}{\nu_r t}\right)^{-\alpha}\right) \quad B$$

Radial Distribution of Stored Charge and Lateral Charge Dissipation.

Experiment examined the radial distribution of charge, and the possibility of lateral charge dispersion over time (TOP). The three figures at left show the normalized spatial profile of the charge for successive discharge times (red) at 60 s, 1 hr and 2 days after deposition and the expected profile of a Gaussian beam with a 5.6 mm FWHM (green) (Bottom). The peak voltage was monitored over time: the amplitude decayed at a rate very similar to that observed in the charge dissipation experiment above. These results suggest dissipation through the thin film and no appreciable lateral diffusion of charge.

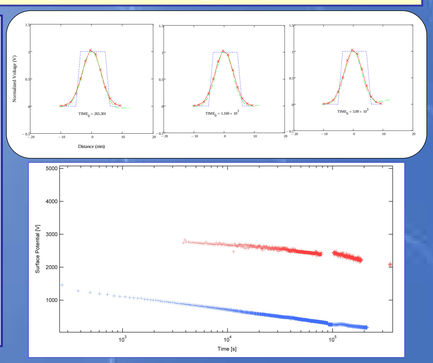

References

Dennison, J. and R. Frederickson, 2002, "Proposal for Measurements of Charge Storage Decay Time and Resistivity of Spacecraft Insulators" in *NASA Space Environments and Effects Kickoff Meeting, San Diego, CA.*

Frederickson, A., C. Benson, and J. Bockman,2003,"Measurement of Charge Storage and Leakage in Polyimides," Nuclear Inst. and Methods in Physics Research, B 208, 454.

Frederickson, A. and J. Dennison,2003,"Measurement of Conductivity and Charge Storage in Insulators Related to Spacecraft Charging," Nuclear Science, IEEE Transactions on 50, 2284.

Frederickson, A. R. and J. R. Dennison, 2003, "Measurement of Conductivity and Charge Storage in Insulators Related to Spacecraft Charging" in *Proceedings of the 2003 IEEE Nuclear and Space Radiation Effects Conference, Monterey, CA.*

Hodges, J, 2010, MS Thesis, Utah State University.

Hoffmann, R., 2010, MS Thesis, Utah State University.

Sim, A, 2010, *11th SCTC Poster Session.*

Swaminathan, P., 2004, MS Thesis, Utah Ste University.

Research was supported by the United States Air Force PALACE Acquire program and funding from the NASA/JWST Electrical Systems Working Group at Goddard Space Flight Center.